

## An Early-Stage Exploration Update on the Grover Point Blind Geothermal System in Dixie Valley, Nevada: Highlights of Geophysics Results and Conceptual Modeling

Matthew Folsom<sup>1</sup>, Carmen Winn<sup>1</sup>, Alex Milton<sup>1</sup>, Jade Zimmerman<sup>2</sup>, Kelly Blake<sup>3</sup>, Andrew Sabin<sup>2</sup>, Christine Downs<sup>4</sup>, Steve Sewell<sup>5</sup>, Kurt Kraal<sup>4</sup>, Stephanie Nale<sup>2</sup>, Wei-Chuang Huang<sup>2</sup>, Paul Schwering<sup>4</sup>

<sup>1</sup>Geological Geothermal Group Inc, 75 Caliente, Reno NV, 89509

<sup>2</sup>Navy Geothermal Program Office, 429 E Bowen Rd., China Lake CA, 93555

<sup>3</sup>Ormat Technologies Inc, 6140 Plumas Street, Reno NV, 89519

<sup>4</sup>Sandia National Laboratories, 1515 Eubank Blvd SE, Albuquerque, NM 87123

<sup>5</sup>Australis Geoscience Ltd. 13 Miro St, Eastbourne, 5013, New Zealand

E-mail: [mfolsom@geologica.net](mailto:mfolsom@geologica.net)

**Keywords:** Geothermal, exploration, geophysics, resistivity, HTEM, gravity methods, geochemistry, LiDAR, blind geothermal systems

### ABSTRACT

The thermal anomaly at Grover Point was first identified by gradient wells in the 1970's where a maximum measured temperature of 72.6°C at 88 meters depth was recorded. It was listed as part of a known geothermal area called Clan Alpine Ranch in the early 2000s and later characterized as associated with a fault step-over in the 2010s by the Nevada Bureau of Mines and Geology at University of Nevada Reno. In 2022, the DOE-funded BRIDGE project (Basin and Range Investigations for Developing Geothermal Energy) flew a network of airborne resistivity surveys over Dixie Valley, Nevada and other prospective areas in the Basin and Range. Shallow low-resistivity zones were identified in several profiles of this geothermal area, referred to as Grover Point in this study, that were consistent with geothermal clay alteration of poorly consolidated sediments over and adjacent to a previously unmapped northeast-striking, northwest-dipping normal fault. Deeper low resistivity zones were also detected, but close to the limits of the method's depth of investigation. This inspired follow-up exploration activities including LiDAR analysis, a 2-meter temperature survey, geochemical sampling of nearby wells, analysis of existing airborne magnetic data, and the collection of a 110-station gravity survey. The preliminary results of this study further define the conceptual elements of a blind geothermal system through the BRIDGE project's research in exploration methodology and conceptual modeling. This workflow is being developed and applied by BRIDGE in the interest of providing the geothermal energy community with cost-effective exploration tools for efficient discovery of blind geothermal systems.

### 1. INTRODUCTION AND OVERVIEW

#### 1.1 Blind Geothermal Systems and the BRIDGE Project

As hydrothermal reservoirs that have explicit surface manifestations are developed for power generation, geothermal resource exploration has increasingly focused on "blind" systems, enhanced geothermal systems, and lower temperature systems. Blind geothermal systems – hydrothermal energy reservoirs lacking typical surface manifestations like hot springs and recent sinter deposition – represent a potentially prolific energy resource that could support critical U.S. public and government energy priorities (e.g., Coolbaugh et al., 2006). The search for blind systems, however, is typically time- and resource-intensive because of its scale. For example, Play Fairway Analysis (PFA), adapted from petroleum and mining exploration, identifies potential locations of hydrothermal systems and qualifies geothermal opportunities by incorporating regional or basin-wide distributions of geochemical, geophysical and geological factors expected to be indicative of favorable heat, permeability, and fluid characteristics. To follow up the success of PFA studies in identifying blind geothermal systems and characterizing prospect favorability in the Great Basin region (e.g., Faulds et al., 2018), the U.S. Department of Energy solicited proposals to further characterize geothermal resource targets suitable for drilling.

The Basin and Range Investigations for Developing Geothermal Energy (BRIDGE) Project kicked off in the Autumn of 2021 (Schwering et al., 2022). The BRIDGE Team is a multi-disciplinary collaboration of subject matter experts being led by Sandia National Laboratories with partners from Geologica Geothermal Group, the US Navy Geothermal Program Office, and independent contractors. The Department of Energy Geothermal Technologies Office (GTO) funded BRIDGE as part of a broader GTO initiative to advance the identification and development of hidden geothermal energy resources in the Basin and Range Province of the western USA. The focus of the BRIDGE project is on western Nevada with areas of interest, identified chiefly from the prior Nevada PFA study (e.g., Faulds et al., 2018), that span both public-use and Department of Defense (DOD) lands.

The BRIDGE workflow, described by Downs et al. (2023), is broadly comprised of five phases: (1) review of existing data and identification of areas of interest, (2) prospect exploration, (3) prospect characterization, (4) temperature confirmation, and (5) resource testing. As costs increase substantially from phase-to-phase, the goal is to make each phase effective in reducing uncertainty and mitigating exploration risk. Area of interest reconnaissance makes use of existing PFA and other data to identify target areas for airborne electromagnetic (AEM) surveying. Incorporation of AEM enables rapid and efficient assessment of potential resources, and helps inform

the planning and design of additional geoscientific investigations. The resulting prospect portfolio may then be iteratively evaluated to prioritize prospects and plan increasingly detailed surveys to characterize the resources. Initial conceptual resource models are then utilized to target shallow temperature wells to confirm subsurface thermal characteristics and calibrate/update conceptual models. Sufficiently favorable resources may then be tested with exploration boreholes.

As part of the overall goals, the BRIDGE program has focused on developing a workflow to effectively incorporate AEM resistivity methods at an early-stage into geothermal exploration in the Basin and Range. The Grover Point prospect illustrates the integration of AEM with other geoscience tools, and demonstrates the utility of collecting this type of data early on in an exploration workflow.

## 1.2 Grover Point Background

The Grover Point prospect is on the eastern side of Dixie Valley and was first identified by temperature gradient hole (TGH) drilling in the late 1970s. The hottest of these wells recorded a bottom hole temperature (BHT) of 72.6°C at 88 m depth, but several wells contributed to a larger region of elevated thermal gradients referred to as the Clan Alpine Ranch (Blackwell et.al., 2007). The geothermal system at Grover Point is one of several systems found in Dixie Valley (DV) (Coolbaugh et al., 2005). These include the Dixie Valley Geothermal Power Plant (DVPP), A drilled and commercially ready prospect at Dixie Meadows, and prospects in various stages of exploration such as Elevenmile Canyon, Pirouette Mountain, Dixie Comstock, and The Bend (Figure 1). Geothermal systems are found throughout Dixie Valley and the Basin and Range at fault terminations and stepovers (Hinz et al., 2014; Faulds et al., 2021). The Tungsten Mountain geothermal power plant is found 25 km to the east of Grover Point, and is the closest commercially operational field.

A large portion of DV was covered by the AEM survey designed and commissioned by BRIDGE (Figure 1). There are many configurations available for AEM surveying. To optimally meet the objectives for this terrain and application, a helicopter-borne transient electromagnetic (HTEM) system was deployed. The HTEM dataset was considered alongside existing public data to help identify prospects for further characterization. Out of several BRIDGE portfolio prospects covered by the HTEM survey in DV, Grover Point was selected for further studies based largely on interpretations of the low-resistivity anomalies imaged by HTEM.

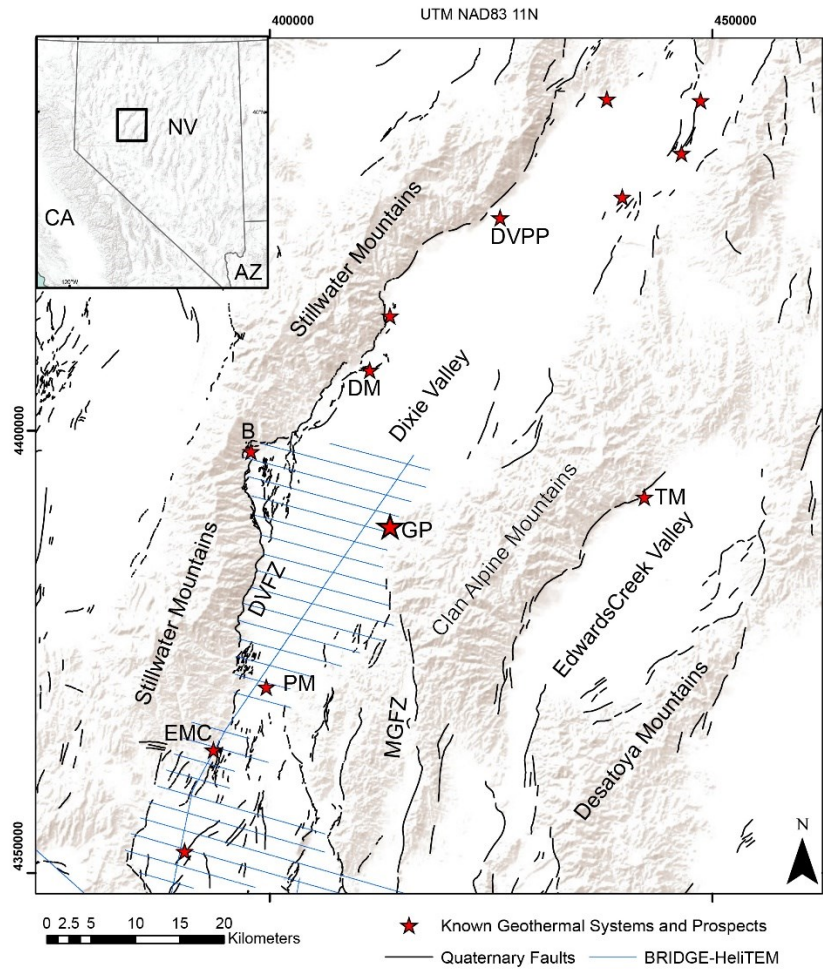


**Figure 1: Location of Dixie Valley including known and prospective geothermal systems including Quaternary faults (dePolo et al., 2008, black lines), and physiographic locations mentioned in the text. DVFZ is Dixie Valley Fault Zone, MGFZ is Middlegate Fault Zone, GP is Grover Point, DVPP is Dixie Valley geothermal power plant, DM is Dixie Meadows, B is the Bend, TM is Tungsten Mountain, PM is Pirouette Mountain, and EMC is Eleven Mile Canyon. HTEM lines collected as part of the BRIDGE project are shown as blue lines. Top left insert: Location of map relative to Nevada state boundary.**

## 2. GEOLOGIC FRAMEWORK

Dixie Valley is bounded to the south by an accommodation zone between DV and Fairview Valley, to the west by the Dixie Valley Fault system (east-dipping, dextral-normal slip) along the Stillwater Range, and to the east by a west-dipping fault system along the Clan Alpine Mountains (Bell et al., 2009). Moderate local strain rates for the region (10-9/yr, Kreemer, 2012) coincide with the extensional regional stress regime and, locally, 0.3-0.5 mm/yr extension rates for Dixie Valley (Hammond et al., 2007). The Stratigraphic sequence includes middle Miocene to present sedimentary and volcanic deposits filling the basin which overlays early to middle Tertiary volcanic rocks and Mesozoic metasedimentary and metavolcanic basement (e.g., Alm 2016).

The Grover Point thermal anomaly is located roughly at the projected intersection of the north-striking, west-dipping Middlegate Fault Zone (MGFZ) and a series of the north-east striking, west-dipping normal faults that lie along the eastern margin of Dixie Valley. Although neither of these fault zones are shown to extend to the thermal anomaly proper (Figure 1), new LiDAR analysis and other work in this report suggests that both zones may extend into this area. Exactly how they interact in the context of the geothermal prospect remains largely unknown.

## 3. HYDROTHERMAL DATA

There are numerous shallow wells and springs near Grover Point that have been logged/sampled for hydrothermal characterization purposes. This section describes the thermal and geochemical data from these sources.

### 3.1 Thermal Data

Shallow artesian wells in the middle of the basin, drilled to depths less than 200 m (although several are deeper), and are associated with an abandoned settlement in the area. Shallow TGH exploration drilling was conducted in 1978 - 1979 and can be found in the SMU Heat Flow and Well Data database. Temperature data from the SMU database includes BHT measurements from 19 wells in the vicinity of the so-called 'Grover Point well' on USGS topographic quads, which became the namesake for this prospect (Figure 2). The Grover Point well is labelled as 903-7 in Figure 2 and has the second highest BHT in the area at 38.82°C at 92 m deep. The hottest well, 903-2, reached a BHT of 72.38°C at 88 m depth. A third warm well, 903-6, has a BHT of 33.59°C at 92 m deep. The remaining wells have BHT values below 30°C, and most of them are below 20°C.

Temperature gradients in many of these wells are significantly elevated above background values in Dixie Valley, which averages  $54 \pm 5$  °C/km (Blackwell et al., 2007). Contoured thermal gradient values indicate an anomalous zone with gradients  $> 500$  °C/km at Grover Point, which is caused by well 903-2. Several other wells in this study area have thermal gradients  $> 250$  °C/km (Blackwell et al., 2007). These elevated gradients may be influenced by the shallow outflow of geothermal fluids, which are common in the Basin and Range. If so, it would not be appropriate to project them to great depths. For instance, at Tungsten Mountain, also a blind system, some shallow wells there intercept 124°C outflow and a thermal roll-over at 152 m deep (Delwiche et al., 2018). This rollover is located at a contact between alluvial cover and underlying tuffs. Temperature-depth profiles are not available at Grover Point, and so it is not possible to assess if and how advective effects are playing a role.

Flowing temperatures from artesian wells in the settlement area to the west of Grover Point are between 15°C and 22°C, with warmer temperatures generally found in the eastern portion of the settlement. Of temperature measurements taken in June of 2023 as part of the BRIDGE project (well names with a \* at the end of the name), there is a clear trend of warming temperatures towards the Grover Point thermal anomaly. The Cattle Well measured 20.6°C and the Spouting Well 18°C; wells in between have temperatures between the two.

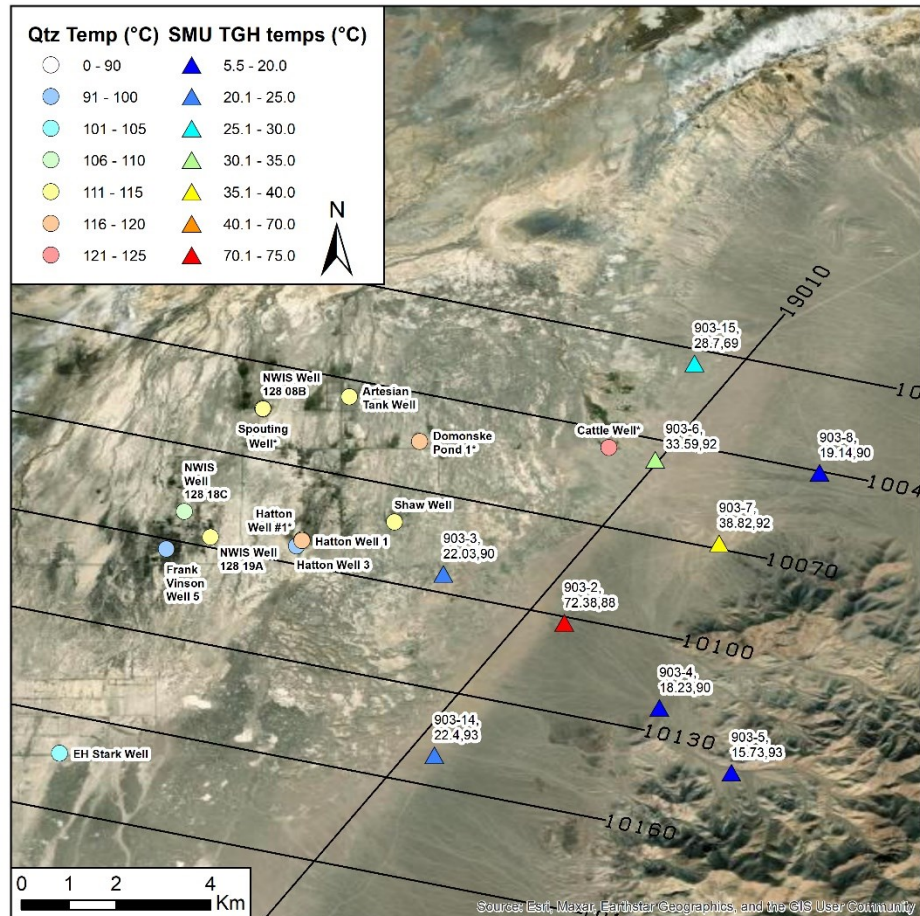


**Figure 2. TGH map near Grover Point (triangles) and geochemistry samples (circles) with HTEM flight lines for reference. Note the greenery in the imagery, indicating the presence of springs and artesian wells.**

### 3.2 Geochemical Data

Geochemical data from approximately ten samples are available near Grover Point in databases like Great Basin Center for Geothermal Energy and Argonne National Laboratory. Of these, only 4 have full analyses of major analytes including bicarbonate. The BRIDGE team collected an additional 4 samples for analysis, including the Cattle Well, Domonske Pond #1, Hatton Well #1, and Spouting Well samples (Figure 2). These waters are Calcium-bicarbonate-sulphate type waters, which are representative of meteoric groundwater in the Basin and Range (Figure 3). While sulphate is commonly found in steam-heated waters from geothermal systems, in the Basin and Range it is also common for the sulphate to be picked up from evaporite-rich basin fill. Chloride concentrations are low (<60 ppm), however, silica concentrations are anomalously high for 20°C water, with quartz geothermometers (conductive, Fournier, 1973) ranging between 92 and 123°C. Similar to the trend with measured temperatures, there is a noticeable trend in the quartz geothermometers of warmer temperatures to the northeast and cooler temperatures to the west and south as distance increases from the thermal anomaly. The Cattle Well sample, which is near well 903-6 (33.59°C), has the highest quartz geothermometry temperature of 123°C. Domonske Pond and Hatton Well 1 both have geothermometry temperatures of 117°C, while samples to the south (such as the EH Stark Well) have temperatures below 100°C. This trend may indicate that trace amounts of geothermal fluid is intermixing with the meteoric groundwater in the region and is consistent with the trend of warmer TGH to the north.

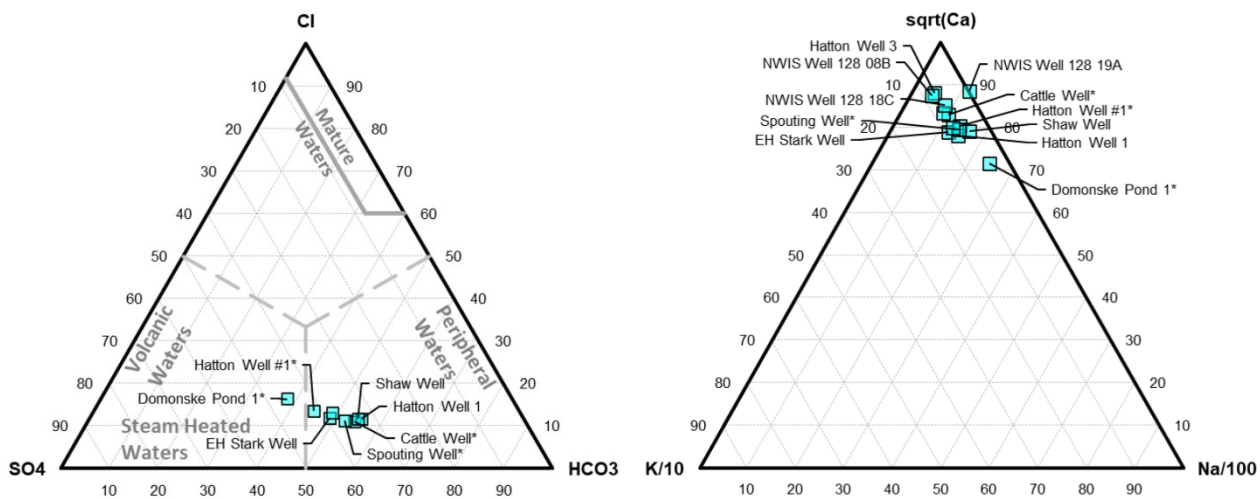


**Figure 3. Geochemical ternary diagrams of the anions (left) and cations (right) of samples from artesian wells near Grover Point. Note that all samples are relatively Calcium (Ca) rich and relatively rich in bicarbonate ( $\text{HCO}_3$ ) and sulphate ( $\text{SO}_4$ ).**

### 4. HTEM

The HTEM resistivity surveying method is typically used for relatively shallow (<500 m depth) mineral exploration and groundwater mapping. The method operates in a similar way to ground-based central loop transient electromagnetic (TEM) surveys. Current is passed through a large wire transmitter loop; the current is turned off and the decay in voltage over time is measured in a small multicoil receiver (X, Y, and Z). The decay in voltage over time is influenced by the subsurface resistivity and hence can be inverted to obtain resistivity with depth information.

As part of the BRIDGE project, HTEM was flown over more than a dozen prospective basins in western Nevada by Xcalibur using their HeliTEM™ system (Sewell et al., 2023). The 7.5 Hz HeliTEM™ system was the most powerful airborne electromagnetic surveying system available to BRIDGE and has been shown to be capable of detecting conductive targets within moderately resistive rocks at depths of over 500 m (Hodges et al., 2016). This survey deployed a transmitter loop with an area 962 m<sup>2</sup>, suspended 35 m above ground, and traveling at an average speed of 110 km/hr. The receiver collected data samples at roughly 10 samples/second, which results in higher lateral resolution than is possible using ground-based methods. The lines and selected segments are shown in map view in Figure 4.

One insightful way to view the HTEM results is to construct a top-of-conductor surface (ToC). The BRIDGE project has separately demonstrated that the elevation of the top of such shallow conductors are correlated with known geothermal prospects in Gabbs Valley and elsewhere. Here we have constructed a ToC grid from the HTEM lines by manually picking the 12 ohm.m contours and gridding the results (Figure 4, colored grid). We note that the ToC is the shallowest in a zone between lines 10100 and 10130, and to the east of tie line 19010.

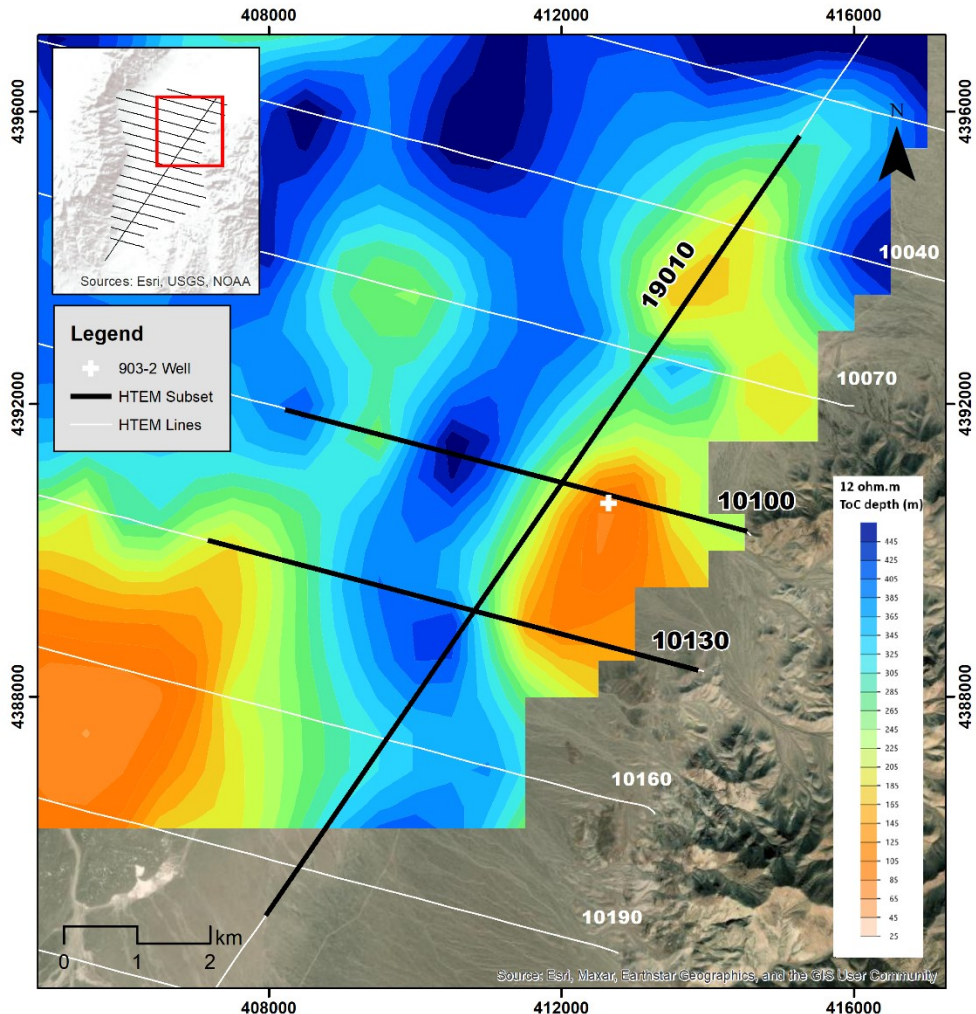


**Figure 4.** Location of HTEM lines in the Grover Point area (white lines) with portions of select cross-sections shown in this paper (black lines). A map of the depth to the top of conductor (ToC), defined as the top of a 12 ohm.m surface, is shown with colored contours.

## 5. 2M TEMPERATURE SURVEY

The 2-meter (2M) temperature survey at Grover Point consists of 64 points collected in one phase in August 2023 and another phase in November 2023 using standard procedures (Coolbaugh et al., 2007, Sladek and Coolbaugh, 2013). Data was collected by the U.S. Navy's Geothermal Program Office. Probes 2.04 m in length were driven into the ground using an electric demolition hammer and temperatures were measured at 1, 1.5 and 2 m depth after they were allowed to equilibrate for a minimum of 1 hour. All point were collected on the shoulders of roadways to minimize the impact of the survey, and the survey design was influenced largely by the distribution of dirt roads. Figure 5 shows images of the survey operations.



**Figure 5. Shallow temperature survey probe installation (left and top right), Resistive temperature device insertion (middle right), and probe retrieval (bottom right).**

Once all of the data points were collected, the temperatures were checked for outliers using a z-score test. No outliers were present in the Grover Point data. Next, these data were corrected for elevation as the survey covered an area with >100 m of elevation change. A datum of 1040 m was chosen for calculating the elevation correction. This was the lowest elevation of all of the probe locations in the dataset. The elevation correction factor ( $Y_t$ ) was calculated using the adiabatic lapse rate of  $1^{\circ}\text{C}/100\text{m}$  where  $X_z$  is the elevation of the probe's location at the ground surface. See Equation 1.

$$Y_t = (1040 \text{ m} - X_z)(-1^{\circ}\text{C}/100 \text{ m}) \quad (1)$$

Equation (1) is applied to each probe location. Calculated  $Y_t$  values were then added to the measured 2M temperature values. Slope and albedo corrections were not applied to these data. To account for the possible seasonal temperature differences between the August and November sampling phases, all data were normalized. To accomplish this, the average background temperature of each phase was calculated. This value was subtracted from the regional background temperature of  $20^{\circ}\text{C}$ , as determined for the Basin and Range by Sladek and Coolbaugh (2013), to obtain the normalization factor for each phase. The calculated normalization factors are  $-6.08^{\circ}\text{C}$  for the August dataset and  $-0.54^{\circ}\text{C}$  for the November dataset. These normalization factors were added to the elevation-corrected values in their respective datasets to generate the final normalized temperatures (Figure 6).

The 2M survey at Grover Point identified a prominent positive temperature anomaly  $\sim 5^{\circ}\text{C}$  above background, with adjusted background temperatures of  $20^{\circ}\text{C}$ . The anomaly is centered near the hot well 903-2. It is roughly 2 km long and 1 km wide in size however, its width east-to-west is poorly constrained.

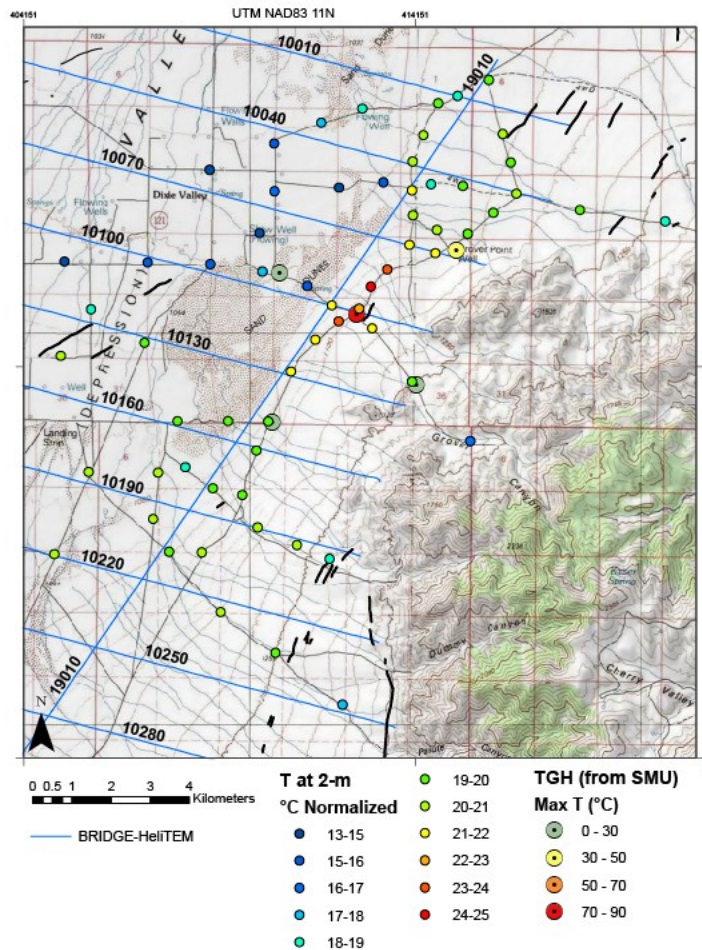


**Figure 6.** Shallow temperature survey results near Grover Point in Dixie Valley are shown as small colored circles. Quaternary faults identified from new analysis of LiDAR data are shown as black lines. HTEM line locations are shown as blue lines. TGH data from the SMU database are shown as larger colored circles.

## 6. POTENTIAL FIELDS

To better understand the structural setting at Grover Point, a new 110-station gravity survey was commissioned and a legacy airborne magnetic dataset was re-examined (USGS OFR, 1985; Alm, 2016).

### 6.1 Gravity

A total of 110 new gravity stations were collected by Zonge International Inc. in the fall of 2023 (Figure 7A). Station spacing varied between 400 m and 800 m to cover a sufficiently large area with the resolution needed for prospect-scale investigation. The survey was designed to characterize the northeast-striking fault zone. The eastern margin of DV is bounded by west dipping structures, but they have not been mapped in this area. A subtle and short (~500 m) Quaternary LiDAR fault scarp was also picked in this vicinity and is shown in Figure 6 - Figure 9.

Using a reduction density of 2.45 g/cc, the complete Bouguer anomaly (CBA) was gridded at 150 m using a minimum curvature algorithm (Figure 7B). An assessment of a suitable reduction density for this area was carried out qualitatively, and an intermediate value of 2.45 g/cc was chosen as a compromise between low-density basin fill and higher-density Paleogene volcanic rocks that comprise the Clan Alpine range. This choice may amplify the gravity values over topographic highs, but it is suitable for investigations under alluvial fans and piedmont slopes where the bulk of Basin and Range geothermal systems are found. Horizontal gradient magnitude (HGM) and first vertical derivative (1VD) grids were produced from the CBA (Figure 7C, D respectively). The CBA was upward-continued by 25 m prior to generating the 1VD grid for smoothing purposes.

The gravity data were modelled in 2D using the GM-SYS profile modeling program, a component of Oasis Montaj software package. The forward gravity response is calculated using methods described by Talwani et al. (1959). A simple, 2-layer model was constructed along HTEM line 10100, which is perpendicular to gravity contours. Densities of 2.12 g/cc and 2.67 g/cc were assigned to the alluvial cover and basement, respectively. No actual measurements of rock densities were taken. The basement contact was modelled dipping gently

from an outcrop on the east to a maximum depth of ~1 km on its western side. Two steep contacts with offsets of ~200 m each helped fit the data where the horizontal gradients were highest. The model fit the data with a root mean square error of ~0.05. Figure 12

## 6.2 Magnetics

The USGS commissioned an aeromagnetic survey over the Clan Alpine Mountains in 1985 (USGS, 1985). The survey was flown along east-west Lines at a survey height of ~300 m, with 800 m line spacing. This data was later re-processed and incorporated with a 2012 aeromagnetic survey commissioned by the U.S. Navy over southern Dixie Valley, using a grid cell size of 100 m. For this study, we clipped out a small subset from these grids and re-applied color scales suitable for this smaller area (Figure 8).

Magnetic data were also collected along each HTEM line, using an in-loop cesium vapor sensor mounted aft of the EM receiver. The nominal height of the sensor was 35 m, much closer to the ground than the 1985 USGS survey. With line spacing of 2 km, however, this survey geometry is suboptimal for gridding the data. This dataset was primarily used for QA/QC of the HTEM data where it is an independent and effective tool for identifying cultural noise. These data were diurnally corrected using a base station and the IGRF removed to provide a residual magnetic intensity (RMI) data channel.

## 6.3 Potential Fields Interpretations

A preliminary structural interpretation has been developed using the gravity and magnetic datasets with context provided by the LiDAR interpretation and the HTEM results (Figure 9). As with many blind geothermal systems in the Basin and Range, some faults at Grover Point may be concealed. In this section we discuss these preliminary geologic interpretations from these potential fields datasets.

Gravity data can be used to delineate the edges of buried, near-vertical contacts using the horizontal gradient method, (Cordell, 1979; Cordell and Grauch, 1985), which takes advantage of the fact that the steepest horizontal gradients in gravity data occur directly over such contacts. We have applied this technique to the Grover Point dataset and made several picks of inferred, steeply-dipping fault locations. The colored grid in Figure 9 shows the gravity HGM of the CBA along with inferred normal fault contacts (black dashed lines). The contours are from the RTP magnetic dataset for comparison purposes. The strongest HGM gradients run north-south before taking a sharp bend to the northeast roughly between HTEM lines 10100 and 10130. This north striking lineament also extends past the bend before also turning northeast and re-connecting to the main HGM lineament. We have less confidence in these more basin-ward features and display them as queried faults in Figure 9. Overall, the patterns suggest that a fault intersection and sharp ~45° bend in faulting is located near the shallow 2M thermal anomaly. It should be noted that the gravity data is only sensitive to faults that host a lateral change in density, and other features would not be detected.

The first vertical derivative (1VD) of potential field data removes regional trends and emphasizes shallower features, as shown by the higher values of the 1VD of the gravity in Figure 7D and the magnetic data in Figure 8D. On the foot-wall side of the fault bend, it is apparent that a high-density and highly magnetized body lies buried at relatively shallow depths and may also outcrop in the range.

The 1VD of the gravity data also suggests that a more basin-ward, near-surface dense body lies ~1.5 km northeast of well 903-2 (Figure 7D). This zone lies between the two inferred northeast-striking normal fault zones. It may be locally caused by a shallowly-buried and down dropped bench in the basement rocks, or possibly by a transition from unwelded to welded tuffs which are both common in this part of the Clan Alpine Range. Given its proximity to inferred geothermal outflow, it is also possible that it results from silicification and densification of sediments, which has been observed at other geothermal fields including San Emidio (Folsom et al., 2020), Don A. Campbell (Orenstein and Delwiche, 2013; Winn et al., 2021) and others. Some types of epithermal silicification processes can occur at shallow depths where geothermal outflow is at the water table (e.g., Hedenquist et al., 2000, and many others).

Evidence for faulting is suggested from a short-wavelength lineament of low magnetic intensity with a northeast strike, which is co-located with the strong gravity HGM lineament picked as a normal fault. This zone is best seen in the RTP of the magnetic data (Figure 8B, contours in Figure 9), and also, in the vertical derivative of the RTP where this feature is emphasized (Figure 8C). Identification of faults buried under alluvial cover using magnetic methods is well documented in Dixie Valley and in other extensional environments (Grauch 2002; Grauch et al., 2001). Alternatively, zones of low magnetic intensity are sometimes observed over parts of geothermal systems and have been attributed to the destruction of magnetic minerals through geothermal processes (Soengkono, 2016). This has been observed at some Basin and Range geothermal systems including Dixie Meadows (Delwiche et al., 2023), the Don A. Campbell operating field (Orenstein and Delwiche, 2013) and at a blind geothermal prospect in South Gabbs Valley (Craig et al., 2021). In addition to these possible explanations, the magnetic low lineament may also be explained by edge-effect from the adjacency of a highly magnetized, shallowly buried lithology, or simply from terrain effects.

A long wavelength trend is also apparent from the magnetic data. This is seen in the RTP grid where magnetization values are lower to the north and higher to the south, separated along a southeastern trend. This entire dataset (Alm, 2016) shows that this zone of low magnetization extends over the entire Clan Alpine Range. This is likely caused by rock units of lower or reverse remnant magnetization that are regionally extensive.

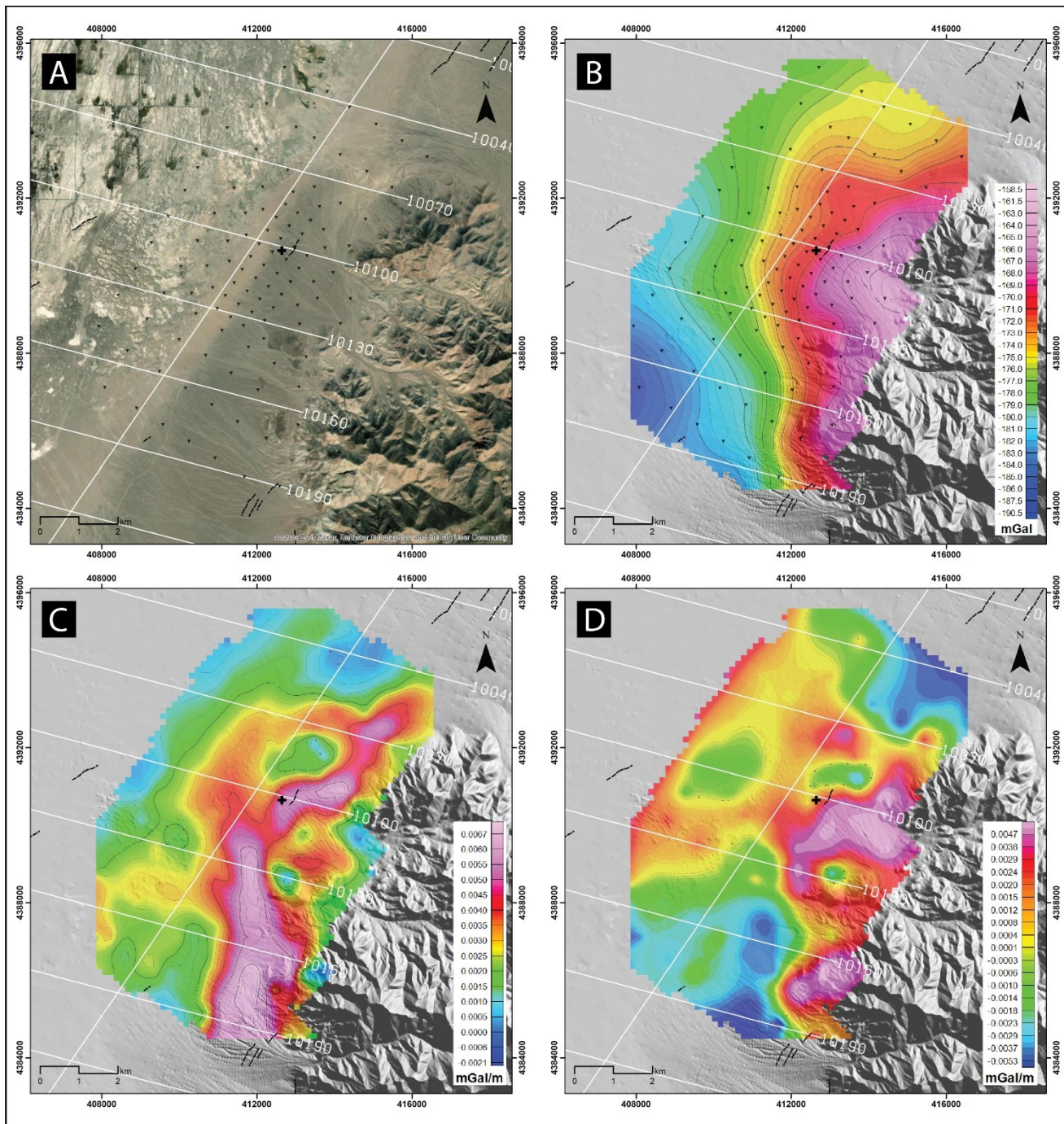


**Figure 7. Gravity survey and results.** LiDAR fault scarps are shown as solid black lines and the hot SMU wellhead location is shown as a black cross. HTEM flight lines (white lines) are shown for reference. Gravity stations are shown as inverted black triangles in Panels A and B. Panel A: Imagery. Panel B: CBA reduced at 2.45 g/cc, gridded at 150 m cell size. Panel C: Horizontal gradient magnitude (HGM) of the CBA. Panel D: First vertical derivative (1VD) of the CBA, first upward continued by 25 m.

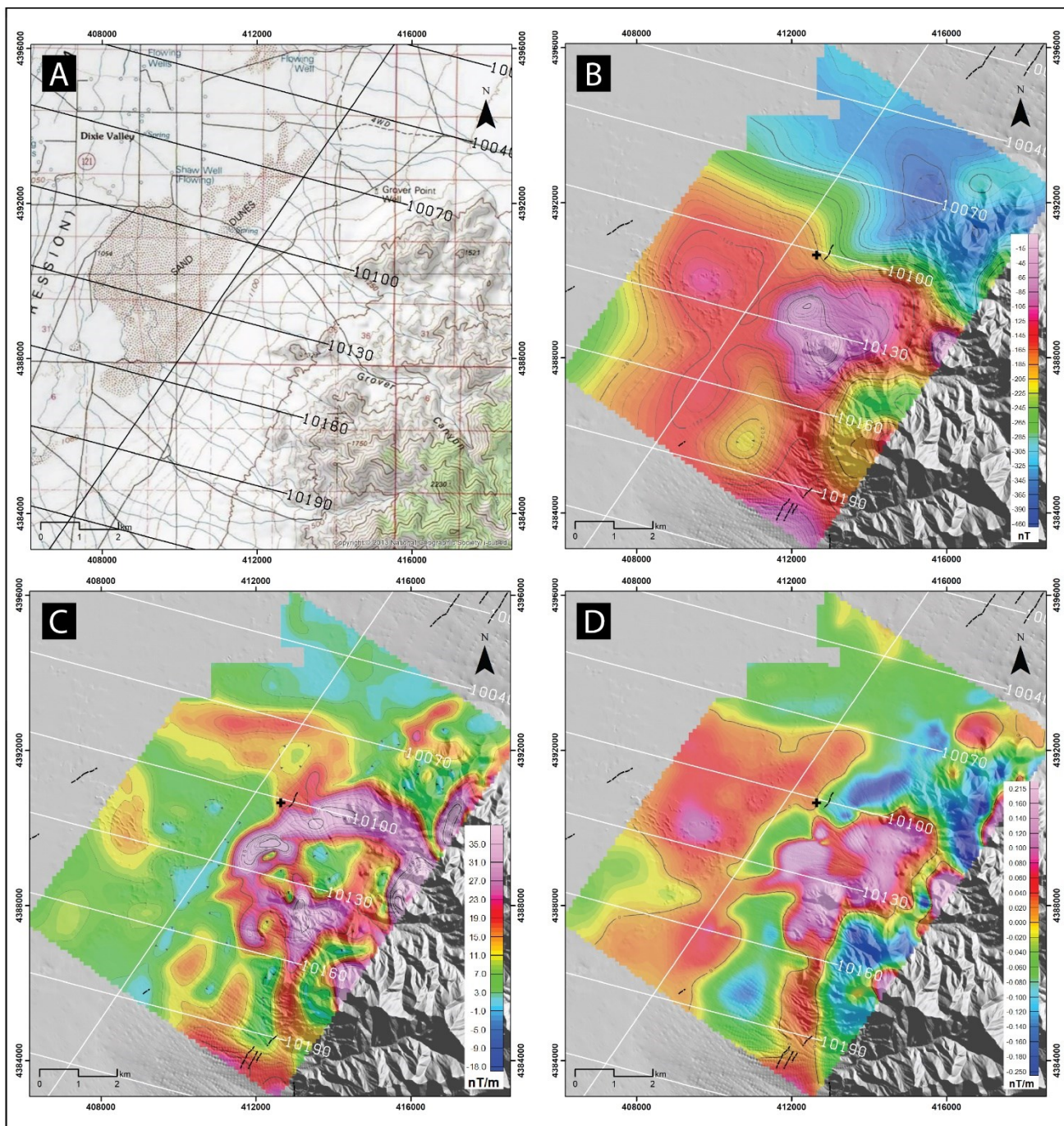


**Figure 8.** A subset of an aeromagnetic survey, flight lines not shown, over the Clan Alpine Mountains (USGS, 1985). On each map, LiDAR fault scarps are shown as solid black lines and the hot SMU well 903-2 is shown as a black cross. HTEM flight lines (white lines) are shown for reference. Panel A: Topographic map; Panel B: Reduced-to-Pole (RTP) magnetic anomaly, Panel C: Horizontal gradient of the RTP anomaly, Panel D: vertical derivative of the RTP anomaly.

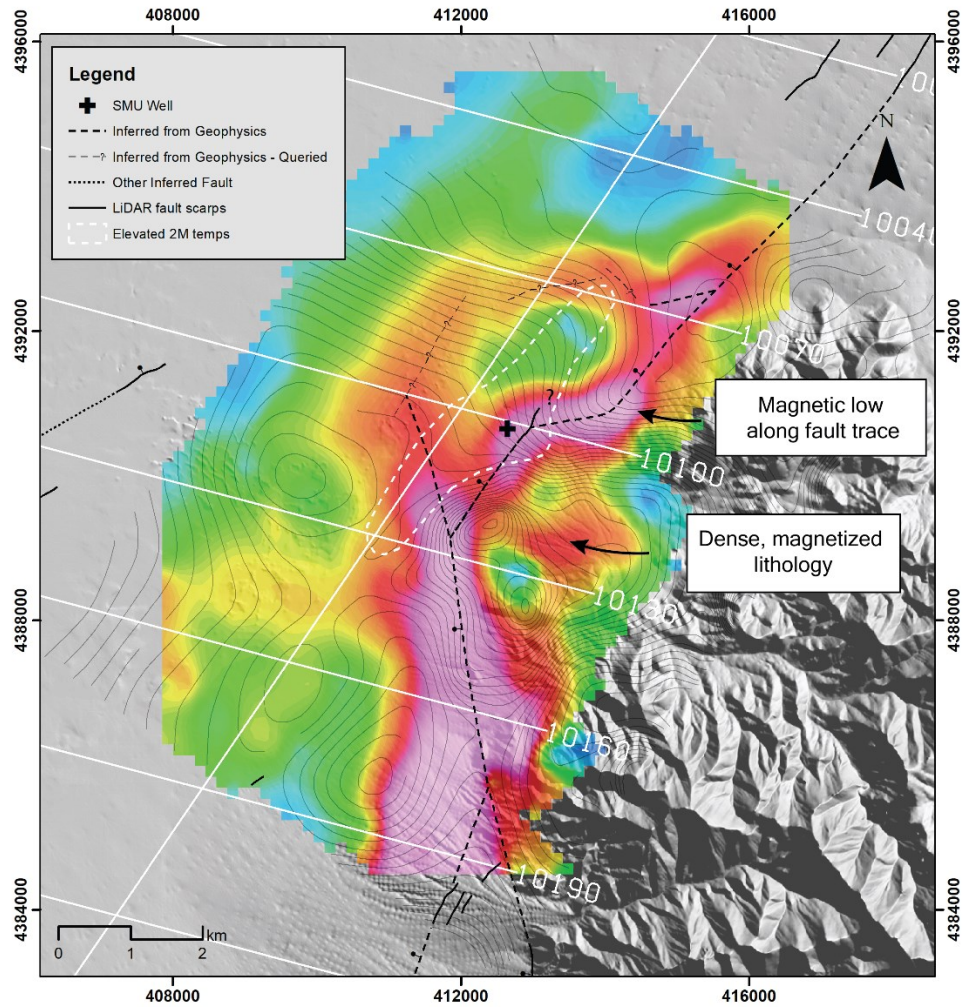


**Figure 9. Preliminary structural interpretations from the gravity and magnetic datasets at Grover Point. Colored grid is the HGM of the gravity CBA. Contours are from the RTP magnetic data. HTEM lines shown as white lines, for reference. A zone of elevated 2M temperatures is highlighted with a dashed white polygon.**

## 7. PRELIMINARY INTERPRETATION AND CONCEPTUAL MODEL

This section describes the preliminary interpretations and conceptual model for the Grover Point geothermal prospect.

### 7.1 Preliminary Interpretation

Figure 10 shows HTEM results in cross-section view along with the RMI collected from an independent magnetometer inside the HTEM loop, and the HGM of the ground-based gravity data, extracted along each line. Also noted on each cross-section is the approximate extent of two-meter temperature (2M) anomalies, the HTEM lines that cross it, and shallow TGH data listing the well name and bottom hole temperature.

Analysis of the BRIDGE HTEM data indicates typical depths of resolution of 300-500 m throughout the basins except where near-surface evaporite deposits and high salinity waters lower resistivity to  $<1$  ohm.m which limits the depth of penetration to  $<100$  m (Sewell et al., 2023). We show the modeling results using a 'standard depth-of-investigation', which is a depth cut-off determined by the inversion program. This cutoff can be seen in the cross sections of Figure 10 where the resistivity colors change from opaque to transparent. HTEM models above this depth cut-off has proven to agree with resistivity models from MT data, and with wells at other locations. Below the computed standard depth of investigation, the resistivity is shown to a constant depth of  $\sim 600$  m. Inverse results in this portion of the models may not be well constrained.

The HTEM surveying at Grover Point identified a low resistivity zone ( $<15$  ohm.m) that encompasses the shallow thermal anomaly identified from well 903-2 and 2M temperature surveying (Figure 10). The top of this low resistivity zone shallows from west to east with near constant dip, consistent with deepening sediments to the west. Where the zone of low resistivity is at its shallowest, it overlies a resistive lens-shaped feature seen on lines 10100 and 10130. The shallow low resistivity zone terminates abruptly on both lines on their eastern sides.

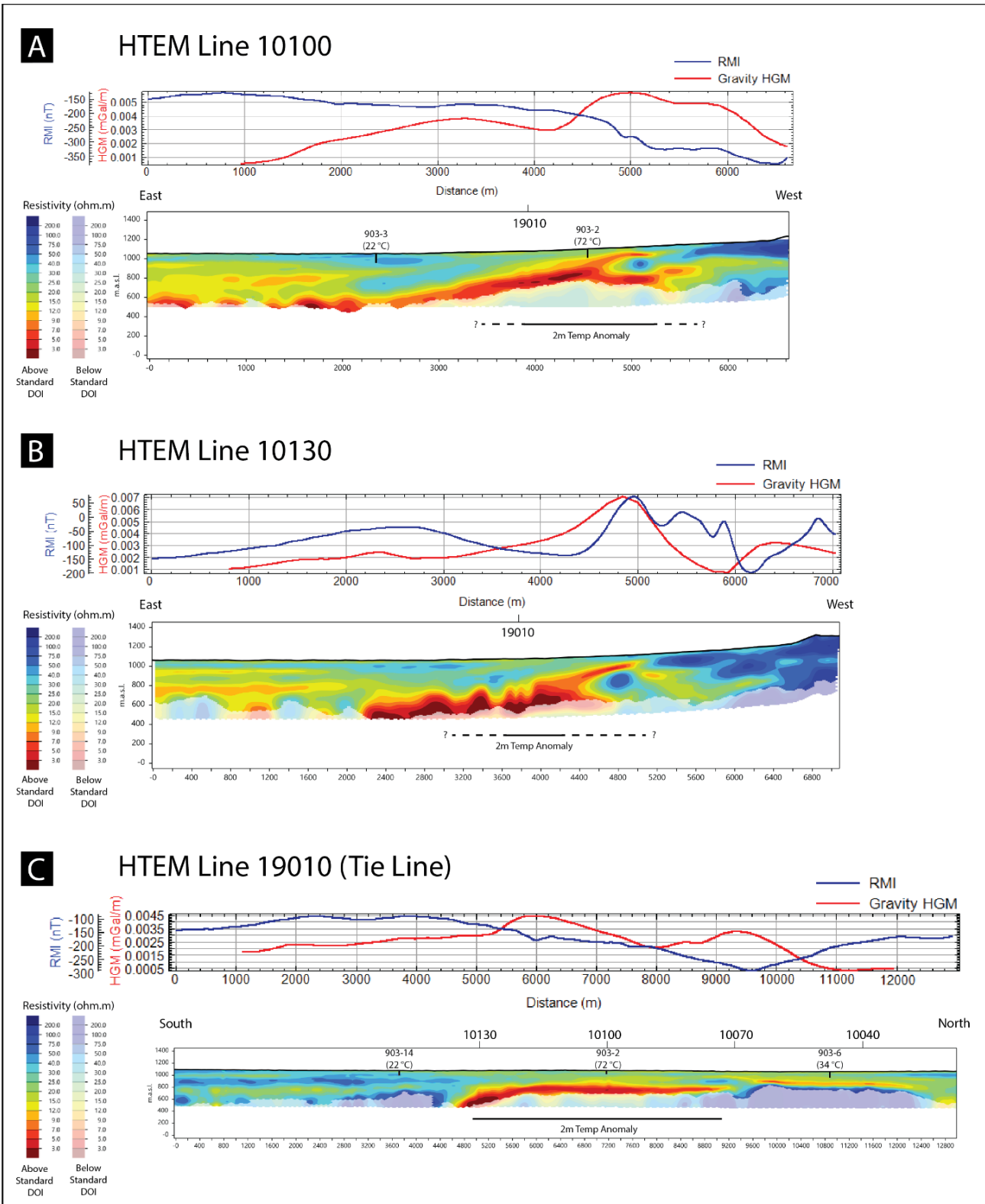


**Figure 10. HTEM resistivity, residual magnetic intensity (RMI) and gravity horizontal gradient magnitude (HGM) extracted along profiles 10100, 10130 and 19020. Zones of elevated 2M temperatures are shown as black lines (solid or dashed) below each resistivity profile. Well names and bottom hole temperatures are shown above each resistivity profile. HTEM lines that cross each profile are noted with the line name.**

We interpret this thin, near-surface conductor co-located with a shallow thermal anomaly as clay alteration within sediments that caps a shallow outflow plume of hot water hosted in the underlying resistive lens. A deeper conductor below the resistive lens is observed on

profiles 10100 and 10130. On the easternmost sections of profiles 10100 and 10130, resistivity is mostly high ( $>50$  ohm.m) consistent with basement rocks in the footwall of a basin-bounding fault. Where the resistivities are the lowest on these profiles, ( $<5$  ohm.m) the DOI is reduced and the base of these contacts cannot be imaged with HTEM. Along line 10130 in particular, the strong deep conductor has an undulating shape, which may not represent the true structure.

HTEM tie line 19010 shows a strong zone of low resistivity at a constant depth and  $\sim 4$  km in length. This zone truncates sharply to the southwest of line 10130 but extends for nearly 2 km northeast of line 10100 and thins in this direction. One possible explanation for this flat-topped geometry is that this profile is parallel to the strike of controlling faults.

## 7.2 Preliminary Conceptual Model

The overall interpretation is that Grover Point lies at the intersection and possible termination of the north-striking MGFZ with northeast-striking normal faults that bound the eastern side of Dixie Valley. This forms a complex structural zone where these two zones meet, which likely influences the presence of a blind geothermal system hosted along a northeast-striking, northwest-dipping normal fault system. Figure 11 shows the conceptual model in map view, noting the extent of an inferred low-resistivity clay ‘cap’, a possible zone of up-flow, and the direction of inferred outflow. The conceptual model is shown in cross section view in Figure 12 and along HTEM line 10100. The depth to basement in Figure 12 was calculated from a 2D model of the gravity data.

Key conceptual model elements identified from these data include:

- The HTEM identified a pattern of resistivity analogous to other producing geothermal systems throughout the Basin and Range (e.g., San Emidio, Brady’s, Desert Peak, Dixie Meadows, Tungsten Mountain) with zones of low resistivity smectite clay alteration in basin-fill sediments capping hot, relatively resistive aquifers. The geometry of the resistivity patterns supports that the system is hosted along northeast-striking faults. The low resistivity zones appear to cap both a deeper semi-confined reservoir and also a shallow, northeast-trending outflow plume. A resistive lens seen best in HTEM line 10100 may indicate a silicified and permeable zone of sediments that helps channelize fluid flow along-strike, as similar features do at other fields. HTEM tie-line 19010 supports an along-strike length of the system potentially up to  $\sim 4$  km, which is similar to many other Basin and Range fields.
- The gravity survey has identified likely fault geometries and can estimate the depth of basin fill. The data is the strongest evidence for the termination of a north-striking, west-dipping fault zone into northeast-striking, northwest-dipping normal faults that bound the eastern margin of DV. These observations are supported by the newly analyzed LiDAR and the legacy aeromagnetic datasets.
- Geochemical analysis identified dilute geothermal fluids with silica geothermometry of  $120^{\circ}\text{C}$  to the north and west of the thermal anomaly. These samples are mixed with meteoric waters which reduces the geothermometry estimates of the maximum temperature of water-rock equilibrium. Maximum reservoir temperatures are unconstrained; however, the patterns of resistivity are similar to other geothermal systems with proven reservoir temperatures in the range of  $135 - 165^{\circ}\text{C}$ .
- Well 903-2 has a BHT of  $72.4^{\circ}\text{C}$  at a depth of 88 m, and a thermal gradient  $> 500^{\circ}\text{C}/\text{km}$ . Given these observations, we assume this well is likely near the hot geothermal up-flow; alternatively, it may be associated with outflow. Additional anomalously warm TGH wells (903-6, 903-7, and 903-15) support outflow to the northeast. The 2M temperature probe survey identified a northeast-trending anomaly directly over inferred faults. Zones with anomalous 2M temperatures are common over shallow outflow plumes, but can be difficult to observe directly over up-flow zones and productive reservoirs where the cap is thicker. We interpret the 2M anomaly at this prospect to represent where these fluids rise to their shallowest depths, along a northeast-flowing outflow path. Limited outflow may move westward where it interacts with shallow groundwaters and provides a geochemical influence, but a limited thermal influence.

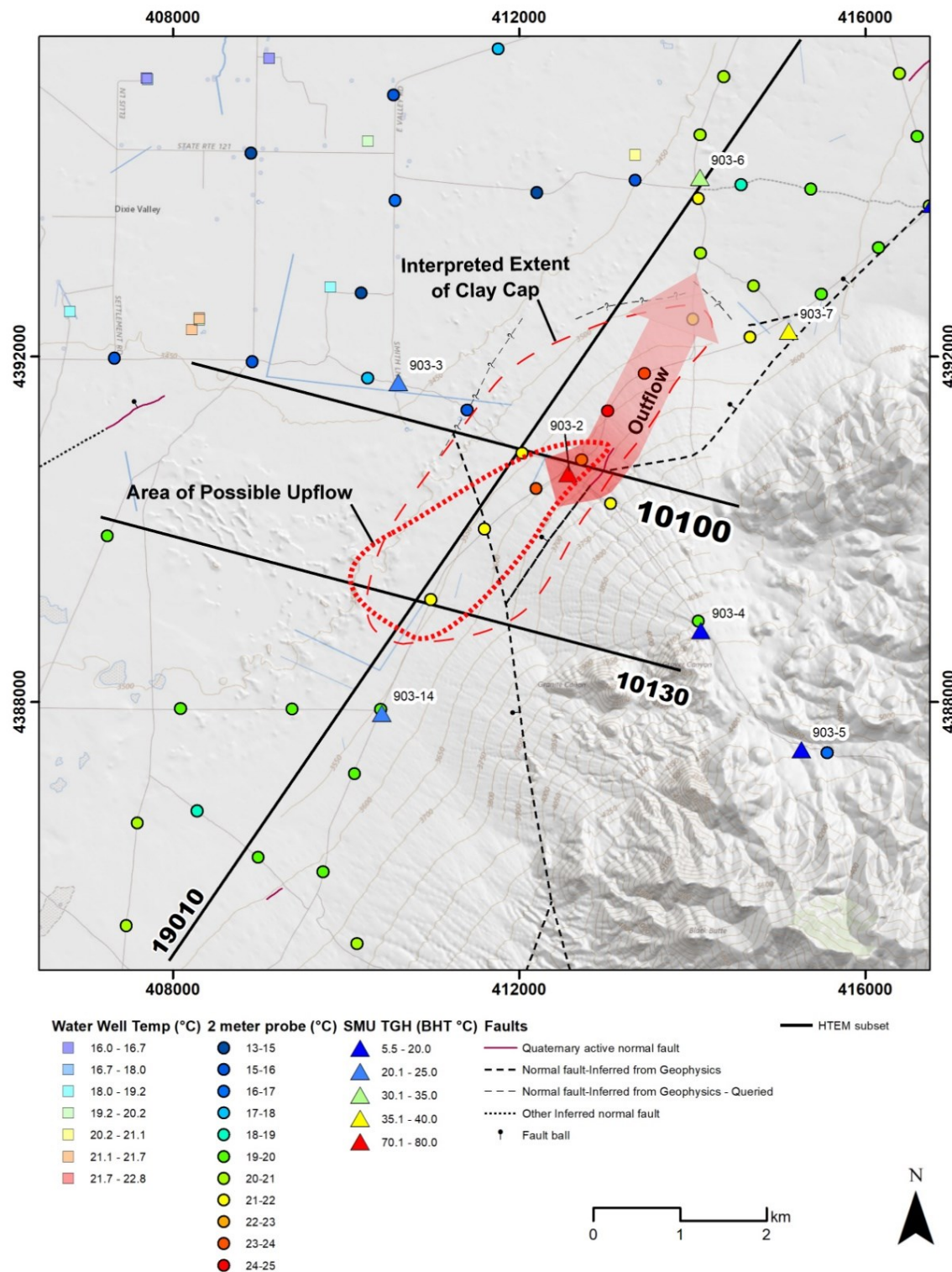
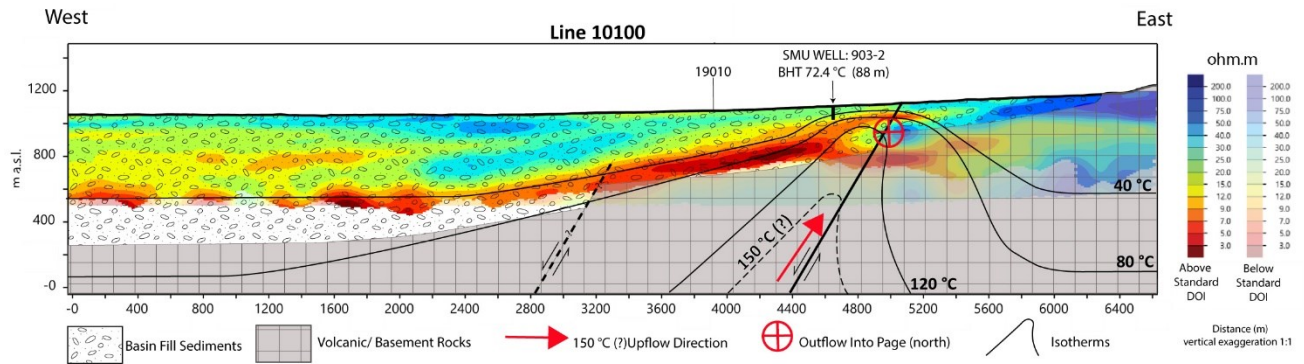


Figure 11. Map view of the conceptual model, with select HTEM lines, temperature data, fault interpretations from gravity, and the inferred outflow.



**Figure 12. Conceptual model cross-section along HTEM profile 10100. HTEM resistivity values are shown as the background colors. The basement – alluvial contact was derived from a 2D gravity model using a density contrast of 0.55 g/cc.**

## 8. CONCLUSION

The Grover Point case study presented here provides an example of the BRIDGE methodology being developed to identify and characterize blind geothermal systems. Work done thus far at Grover Point has progressed the prospect from a limited thermal anomaly to a conceptual model that supports the existence of a potentially power capable resource. Further work is needed to prove this system, particularly TGH drilling to indicate that resource temperatures  $>120^{\circ}\text{C}$  may exist here. An MT survey is underway that can better characterize the deeper resistivity structure in the area of interest, and a geologic mapping campaign is also in a planning stage. These data will be help further refine the conceptual model and guide the targeting of a future TGH drilling program.

## ACKNOWLEDGEMENTS

This material was based upon work supported by the U.S. Department of Energy, Office of Energy Efficiency and Renewable Energy (EERE), Office of Technology Development, Geothermal Technologies Office under the FY2020 Hydrothermal and Low Temperature Multi-Topic Funding Opportunity Announcement DE-FOA-0002219. Sandia National Laboratories is a multimission laboratory managed and operated by National Technology & Engineering Solutions of Sandia, LLC, a wholly owned subsidiary of Honeywell International Inc., for the U.S. Department of Energy's National Nuclear Security Administration under contract DENA0003525. This paper describes objective technical results and analysis. Any subjective views or opinions that might be expressed in the paper do not necessarily represent the views of the U.S. Department of Energy or the United States Government. The United States Government retains, and the publisher, by accepting the article for publication, acknowledges that the United States Government retains a non-exclusive, paid-up, irrevocable, world-wide license to publish or reproduce the published form of this manuscript, or allow others to do so, for United States Government purposes. The authors appreciate the support and cooperation of the local Bureau of Land Management and Department of Defense agencies for site access. The authors are grateful to the Xcalibur and Heli Carrier team for coordinating and conducting the HeliTEM™ survey safely and effectively, and to Zonge International Inc. for conducting an efficient and effective gravity survey. The authors also thank Paul Bedrosian of the USGS for the EM inversion support.

Finally, we would like to thank our reviewers William Cumming and Nick Hinz for their thoughtful and detailed edits of this paper, which improved it significantly.

## REFERENCES

Alm, S. A. (2016). A Geological and Geophysical Investigation into the Evolution and Potential Exploitation of a Geothermal Resource at the Dixie Valley Training Range, Naval Air Station Fallon (Doctoral dissertation, University of Kansas).

Bell, J. W., Caskey, S. J., & House, P. K. (2009). *Geologic Map of the Lahontan Mountains Quadrangle, Churchill County, Nevada*. Nevada Bureau of Mines and Geology.

Blackwell, D.D., Smith, R.P., & Richards, M.C. (2007). EXPLORATION AND DEVELOPMENT AT DIXIE VALLEY, NEVADA: SUMMARY OF DOE STUDIES.

Coolbaugh, M., and 14 others: Geothermal potential map of the Great Basin, western United States: Nevada Bureau of Mines and Geology Map 151 (2005).

Coolbaugh, M.F., Raines, G.L., Zehner, R.E., Shevenell, L., & Williams, C.F. (2006). Prediction and discovery of new geothermal resources in the Great Basin: multiple evidence of a large undiscovered resource base. *Geotherm. Res. Council Trans.*, 30, pp. 867-874.

Coolbaugh, M. F., Sladek, C., Faulds, J. E., Zehner, R. E., & Oppliger, G. L. (2007, January). Use of rapid temperature measurements at a 2-meter depth to augment deeper temperature gradient drilling. In *Proceedings, thirty-second workshop on geothermal reservoir engineering, Stanford University* (Vol. 8).

Cordell, L. (1979). Sedimentary facies and gravity anomaly across master faults of the Rio Grande rift in New Mexico. *Geology*, 7(4), 201-205.

Cordell, L., & Grauch, V. J. S. (1985). Mapping basement magnetization zones from aeromagnetic data in the San Juan Basin, New Mexico. In *The utility of regional gravity and magnetic anomaly maps* (pp. 181-197). Society of Exploration Geophysicists.

Craig, J. W., Faulds, J. E., Hinz, N. H., Earney, T. E., Schermerhorn, W. D., Siler, D. L., ... & Deoreo, S. B. (2021). Discovery and analysis of a blind geothermal system in southeastern Gabbs Valley, western Nevada, USA. *Geothermics*, 97, 102177.

Delwiche, B., Libbey, R., Folsom, M., Johnson, A., Murphy, J., & Zuza, R. (2023) Exploration History and Conceptual Model of the Dixie Meadows Geothermal Field, Nevada, USA.

Delwiche, B., Peters, B., Sophy, M., Smith, C., & O'Brien, J. (2018, February). Successful deployment of a multi-crossing directional drilling method at Ormat's New tungsten Mountain geothermal Field in Churchill County, Nevada. In *Proceedings, 43rd Workshop on Geothermal Reservoir Engineering*. Stanford University, Stanford, Ca. February.

dePolo, C. M., Johnson, G. L., Price, J. G., & Mauldin, J. M. (2008) Quaternary Faults in Nevada—Online Interactive Map.

Downs, C., Schowering, P. C., Sewell, S., Winn, C., Hinz, N., Zimmerman, J., Blake, K., Sabin, A., Lopeman, J., Milton, A., Siler, D., Cumming, W. (2023). Development of the Prospect Portfolio and Initial Surface Exploration Studies in the Basin & Range Investigations for Developing Geothermal Energy (BRIDGE) Project. *GRC Transactions*, Vol. 47, 2023.

Faulds, J. E., Hinz, N. H., Coolbaugh, M., Avling, B., Glen, J., Craig, J. W., ... & Hardwick, C. (2021). *Discovering Blind Geothermal Systems in the Great Basin Region: An Integrated Geologic and Geophysical Approach for Establishing Geothermal Play Fairways: All Phases* (No. DOE-UNR-06731-01). Univ. of Nevada, Reno, NV (United States); ATLAS Geosciences, Inc., Reno, NV (United States); US Geological Survey, Menlo Park, CA (United States); Hi-Q Geophysical, Inc., Ponca City, OK (United States); Innovate Geothermal Ltd, Vancouver (Canada); Utah Geological Survey, Salt Lake City, UT (United States).

Faulds, J.E., Craig, J.W., Coolbaugh, M.F., Hinz, N.H., Glen, J.M., & Deoreo, S. (2018). Searching for blind geothermal systems utilizing play fairway analysis, western Nevada. *Geotherm. Res. Council Bull.*, 42, pp. 34-42.

Faulds, J., & Hinz, N. (2015, April). Favorable tectonic and structural settings of geothermal systems in the Great Basin region, western USA: Proxies for discovering blind geothermal systems. In *Proceedings World Geothermal Congress*, Melbourne, Australia, 19-25 April 2015 (No. DOE-UNR-06731-02). Nevada Bureau of Mines and Geology, University of Nevada, Reno.

Folsom, M., Libbey, R., Feucht, D., Warren, I., & Garanzini, S. (2020, February). Geophysical Observations and Integrated Conceptual Models of the San Emidio Geothermal Field, Nevada. In *Proceedings of the 45th Workshop on Geothermal Reservoir Engineering*, Stanford University, Stanford, CA, USA 21p.

Grauch, V. J. S. (2002). High-resolution aeromagnetic survey to image shallow faults, Dixie Valley geothermal field, Nevada (pp. 1-13). US Department of the Interior, US Geological Survey.

Grauch, V. J. S., Hudson, M. R., & Minor, S. A. (2001). Aeromagnetic expression of faults that offset basin fill, Albuquerque basin, New Mexico. *Geophysics*, 66(3), 707-720.

Hammond, W. C., Kreemer, C., & Blewitt, G. (2007). Exploring the relationship between geothermal resources and geodetically inferred faults slip rates in the Great Basin. *Geothermal Resources Council Transactions*, 31, 391-395.

Hedenquist, J. W., Arribas, A. N. T. O. N. I. O., & Gonzalez-Urien, E. (2000). Exploration for epithermal gold deposits.

Hinz, N. H., Faulds, J. E., & Coolbaugh, M. F. (2014). Association of fault terminations with fluid flow in the Salt Wells geothermal field, Nevada, USA. *Geothermal Resources Council Transactions*, 38, 3-10.

Hodges, G., Chen, T., van Buren, R., 2016. HeliTEM detects the Lalor VMS deposit. *Exploration Geophysics*, 47:4, 285-289

Kreemer, C., Hammond, W. C., Blewitt, G., Holland, A. A., & Bennett, R. A. (2012, April). A geodetic strain rate model for the Pacific-North American plate boundary, western United States. In *EGU General Assembly Conference Abstracts* (p. 6785).

U.S. Geological Survey (1985). Aeromagnetic map of the Clan Alpine Mountains, west-central Nevada; Open-File Report 85-752. <https://doi.org/10.3133/ofr85752>

Orenstein, R., & Delwiche, B. (2014). The Don A. Campbell Geothermal Project. *Geothermal Resources Council Transactions*, 38, 91-98.

Schwering, P., Lowry, T., Hinz, N., Matson, G., Sabin, A., Blake, K., Zimmerman, J., Sewell, S., & Cumming, W. (2022). The BRIDGE Project – hidden systems reconnaissance in western Nevada. *Geotherm. Res. Council Bull.*, 46, pp. 1145-1158.

Sewell, S., Cumming, W. Schwering, P., Hinz, N., Downs, C., Zimmerman, J., Bedrosian, P., Robinson, B., Murray, D., Schlutz, A. (2023). Using helicopter time-domain electromagnetic (HELIEM) resistivity surveys with supporting geoscience data to target temperature gradient wells and discover hidden geothermal systems in the US Basin and Range. *Geotherm. Res. Council Bull.*, 47

Sladek, C., & Coolbaugh, M. (2013). Development of online map of 2 meter temperatures and methods for normalizing 2 meter temperature data for comparison and initial analysis. *Geothermal Resources Council Transactions*, 37, 333-336.

Soengkono, S. (2016). Airborne magnetic surveys to investigate high temperature geothermal reservoirs. In *Advances in Geothermal Energy* (p. 113). IntechOpen.

Talwani, M., Worzel, J. L., & Landisman, M. (1959). Rapid gravity computations for two-dimensional bodies with application to the Mendocino submarine fracture zone. *Journal of geophysical research*, 64(1), 49-59.

Winn, C., Dobson, P., Ulrich, C., Kneafsey, T., Lowry, T., Akerley, J., ... & Bauer, S. (2021). Lost Circulation in a Hydrothermally Cemented Basin-Fill Reservoir: Don A. Campbell Geothermal Field, Nevada (No. SAND2021-7728C). Sandia National Lab. (SNL-NM), Albuquerque, NM (United States).